MARS ODYSSEY THEMIS OBSERVATIONS OF PHOBOS: NEW SPECTRAL AND THERMOPHYSICAL MEASUREMENTS. J. L. Bandfield[1] , S. Piqueux[2], T. D. Glotch[3], K. A. Shirley[3], T. C. Duxbury[4], J. R. Hill[5], C. S. Edwards[6], J. J. Plaut[2], V. E. Hamilton[7], P. R. Christensen[5], [1]Space Science Institute (jbandfield@spacescience.org), [2]Jet Propulsion Laboratory, California Institute of Technology, [3]Stony Brook University, [4]George Mason University, [5]Arizona State University, [6]Northern Arizona University, [7]Southwest Research Institute.

Introduction: The origin of Phobos and Deimos remains a widely debated topic in planetary science. There are two basic hypotheses for the moons' origin: 1) It is a captured asteroid [e.g., 1,2], or 2) formation *in situ*, either from accretion of ejecta from a large impact, or co-accretion with Mars [e.g., 3,4].

The captured asteroid hypothesis relies primarily on visible and near-infrared (VNIR) spectral and other similarities to primitive D-type asteroids, which are found beyond Mars' orbit [e.g., 5,6]. These bodies have relatively featureless VNIR spectra with red slopes and low albedos, similar to Phobos and Deimos. By contrast, no VNIR spectral features associated with martian crustal or mantle compositions have been detected [6]. However, the nearly circular orbits of Phobos and Deimos near the equatorial plane of Mars are difficult to reconcile with the captured asteroid hypothesis. The orbits are instead consistent with formation of the moons *in situ* via accretion [e.g., 4].

To address these hypotheses and other aspects of its history, Phobos has been studied via spacecraft-based thermal, imaging, spectroscopy, and gravity measurements [e.g., 4,7–9]. To add to this, we have started collecting a series of observations of Phobos using the 2001 Mars Odyssey Thermal Emission Imaging System (THEMIS) [10]. These data are the highest spatial resolution thermal infrared (TIR) observations collected of Phobos to date and systematic data collection is planned to observe the Mars-facing hemisphere of Phobos at a variety of phase angles and local times. These measurements will allow for characterization and mapping of the thermophysical and bulk compositional properties.

THEMIS Phobos Observations: THEMIS collected 10-band TIR and 1-band visible wavelength images near the closest approach of the spacecraft on 29 September 2017, with 1.3 km and 270 m/pixel sampling respectively at nadir (Fig. 1). The TIR measurements include approximately 175 pixels that cover Phobos, from pre-dawn to late morning local times at locations from ~30°S–60°N and ~310°–50°E. Most data with emission angles <60° covered daytime surfaces. This is due to the geometry of the observation combined with the irregular shape of Phobos. Only a few pre-dawn measurements were collected in the southern hemisphere.

TIR data were calibrated using surrounding space as a reference to determine signal offset. Gain settings were derived from pre-flight measurements [10]. This method allowed for a robust removal of line and row correlated noise and focal plane temperature drift effects. Comparison with data calibrated using the internal THEMIS reference flag provided an independent validation of the data accuracy.

Results: THEMIS band 10 (14.8 μm) brightness temperatures range from 139 to 160 K. The spectra have a blue slope and shorter wavelength (7.9 μm) brightness temperatures are higher, ranging from 159 to 274 K. The spectral slopes are present in all data, but are more prominent near the terminator.

In addition to the spectral slopes, the THEMIS data show a broad absorption in emissivity spectra from 8.5–11.0 μm. There is also a steep drop in emissivity at 6.8 μm. No systematic variations in spectral shape are apparent in the data.

Preliminary Interpretations: *Thermophysical Properties.* The THEMIS data provide a view of the

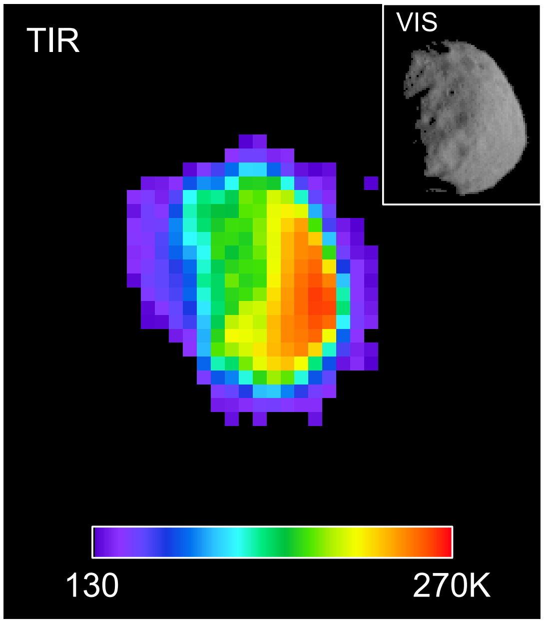

Figure 1. *THEMIS images of Phobos. The TIR image shows the broadband brightness temperature. Phobos' equator runs from the upper left through the lower right and the prime meridian is near the center of the object. Brightness temperatures below 130K (near the uncertainty level of the bolometric temperatures) are masked. The inset shows the visible wavelength image.*

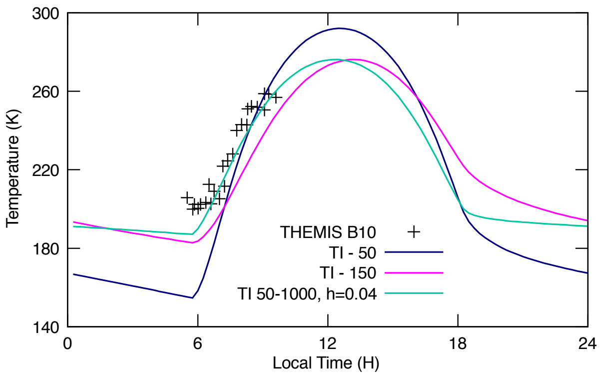

Figure 2. *THEMIS band 10 (14.9 μm) 0–20°N brightness temperatures (black crosses) and predicted temperatures from a thermal model (solid lines). Dark blue and magenta lines show temperatures for vertically uniform materials with a thermal inertia of 50 and 150 J m^{-2} K^{-1} s$^{-½}$ respectively. The cyan line shows predicted temperatures for fine soil over rocky materials, with a thermal inertia varying from 50 at the surface to 1000 at depth (with an h-parameter value of 0.04 m [13]). This model captures the early morning rise in Phobos temperatures.*

warming of Phobos throughout the morning. Equatorial surface band 10 (14.8 μm) brightness temperatures span ~195–260 K from 0600–1030H local times. The warming occurs ~1 hour earlier than predicted using a vertically uniform thermal model and the relatively moderate temperature range indicates the presence of elevated values of thermal inertia.

Although a thermal inertia value of ~150 J m^{-2} K^{-1} s$^{-½}$ is consistent with the range of temperatures and warming rate, it does not predict the early timing of the surface heating. Instead, we can reasonably match the Phobos morning temperatures using a layered model consistent with several centimeters of fluffy regolith that transitions to a rocky substrate (Fig. 3).

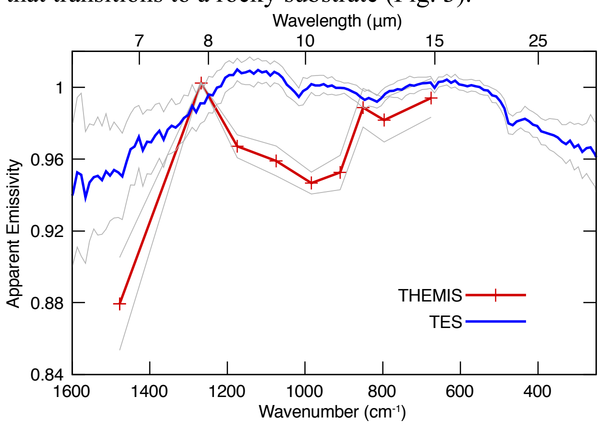

Figure 3. *Average THEMIS (red) and TES (blue) apparent emissivity spectra of Phobos. Both spectra have had continuum slopes removed and standard deviations are shown by gray lines.*

Previous measurements from the Viking Infrared Thermal Mapper (IRTM) were used to derive thermal inertia values of ~25–80 J m^{-2} K^{-1} s$^{-½}$ [7]. Although these values are similar to the surface layer in our best-fit model, the low pre-dawn equatorial temperatures (<150 K) measured by IRTM are inconsistent with the presence of a high thermal inertia substrate.

Spectral Properties. The THEMIS continuum-removed spectra are consistent with silicate-dominated materials. The spectral contrast is similar in magnitude to lunar spectra [12], which are dominated by fine-particulate silicates in a vacuum environment. The wavelengths of the emissivity maximum and the broad absorption in bands 4–7 are also consistent with the presence of materials with an SiO_2 content similar to pyroxene minerals or basaltic rocks, as opposed to more silicic or ultramafic compositions.

The THEMIS spectra do not match data acquired by the Mars Global Surveyor Thermal Emission Spectrometer (TES; Fig. 3) [e.g., 11]. The TES data show absorptions and an emissivity maximum at longer wavelengths, with an overall much lower spectral contrast. Both datasets have significant signal and high radiometric accuracy and the large spectral difference between the two datasets is remarkable. One explanation for this difference is the lack of spatial overlap between the two datasets. The TES data are dominated by Phobos' "blue unit" [6] associated with Stickney crater. The THEMIS data cover Phobos' "red unit" in the eastern hemisphere.

Conclusions: The TIR imaging of Phobos is revealing new spectral and thermophysical properties. THEMIS spectra show evidence for silicate-dominated materials and comparison with previous measurements could indicate significant compositional heterogeneity. In addition, comparison of temperature measurements with thermophysical models are consistent with thermophysically complex layered surface materials. Additional observations are planned to help confirm and refine the initial analyses presented here.

References: [1] Burns, J.A., (1978) *Vistas Astron.*, *22*, 193. [2] Hartmann, W. (1990) *Icarus*, *87*, 236. [3] Safronov, V.S. et al. (1986) In: Burns, J.A., Matthews, M.S. (Eds.), *Satellites*. Univ. Arizona Press, 89. [4] Craddock, R.A. et al. (2011) *Icarus*, *211*, 1150. [5] Murchie, S., S. Erard (1996) *Icarus*, *123*, 63. [6] Fraeman, A.A. et al. (2014) *Icarus*, *229*, 196. [7] Lunine, J.I. et al. (1982) *JGR*, *87*, 10297. [8] Basilevsky, A.T. et al. (2014) *Plan. Space Sci.*, *102*, 95. [9] Pätzold, M. et al. (2014) *Plan. Space Sci.*, *102*, 86. [10] Christensen, P.R. et al. (2004) *SSRv.*, *110*, 85. [11] Glotch, T.D. et al. (2015) *LPSC*, *46*, 2587. [12] Salisbury, J.W. et al. (1985) *Icarus, 115*, 181. Hayne, P.O., et al. (2017), *JGR*, *122*, 10.1002/2017JE005387.